

# SCIENTIFIC REPORTS



OPEN

## miR-140-5p regulates adipocyte differentiation by targeting transforming growth factor- $\beta$ signaling

Received: 27 August 2015  
Accepted: 12 November 2015  
Published: 11 December 2015

Xin Zhang<sup>1,\*</sup>, Ailing Chang<sup>2,\*</sup>, Yongmei Li<sup>1</sup>, Yifei Gao<sup>1</sup>, Haixiao Wang<sup>3</sup>, Zhongshu Ma<sup>2</sup>, Xiaoxia Li<sup>4</sup> & Baoli Wang<sup>1</sup>

Recent emerging studies of miRNAs in adipocyte commitment provide new insights to understand the molecular basis of adipogenesis. The current study indicated that miR-140-5p was altered in primary cultured marrow stromal cells and established progenitor lines after adipogenic and/or osteogenic treatment. miR-140-5p was increased in adipose tissue in db/db obese mice vs. lean mice. Supplementing miR-140-5p activity induced stromal cell ST2 and preadipocyte 3T3-L1 to differentiate into mature adipocytes. Conversely, inhibition of the endogenous miR-140-5p repressed ST2 and 3T3-L1 to fully differentiate. By contrast, knockdown of the endogenous miR-140-5p enhanced osteoblast differentiation. Transforming growth factor- $\beta$  receptor I (Tgfr1) was shown to be a direct target of miR-140-5p. Supplementing miR-140-5p in ST2 reduced the level of TGFBR1 protein, while suppression of endogenous miR-140-5p increased TGFBR1. Overexpression of Tgfr1 inhibited, whereas knockdown of Tgfr1 promoted adipogenic differentiation of ST2 cells. Further investigation of mechanisms that control miR-140-5p expression revealed that C/EBP $\alpha$  induced transcriptional activity of the miR-140-5p promoter. Removal of the putative response element of C/EBP from the promoter abolished the enhancement of the promoter activity by C/EBP $\alpha$ , suggesting that C/EBP $\alpha$  transcriptionally controls miR-140-5p expression. Taken together, our study provides evidences that miR-140-5p regulates adipocyte differentiation through a C/EBP/miR-140-5p/TGFBR1 regulatory feedback loop.

It is believed that adipocyte and osteoblast originate from a common mesenchymal stem cell (MSC), thus a reciprocal and inverse relationship exists between adipogenesis and osteogenesis<sup>1</sup>. Commitment of marrow mesenchymal stem cells to adipocytes is governed by the coordination of peroxisome proliferator-activated receptor  $\gamma$  (PPAR $\gamma$ ) and members of the CCAAT/enhancer binding protein (C/EBP) family<sup>2–5</sup>. *In vivo* and *in vitro* studies have shown that PPAR $\gamma$  is critical both for adipocyte differentiation and for major functions of mature adipocytes, including lipid metabolism, adipokine secretion, and insulin sensitivity<sup>6,7</sup>. Three members of C/EBP family, i.e., C/EBP $\alpha$ , C/EBP $\beta$ , and C/EBP $\delta$ , have been found to work together with PPAR $\gamma$  to fully exert their adipogenic roles<sup>8–12</sup>. Osteogenesis is also a highly coordinated process and is governed by the activation of Wnt/ $\beta$ -catenin signaling and the expression of several master transcription factors including Runt-related transcription factor 2 (Runx2), osteix (Osx) and distal-less homeobox 5 (Dlx5)<sup>13,14</sup>.

Recent emerging studies have shown that miRNAs are able to indirectly regulate adipogenic and/or osteoblast differentiation of MSCs by targeting various genes that may be involved in balancing self-renewal and stem cell differentiation. miRNA family 27 (miR-27a and miR-27b) has been found to be able to negatively regulate adipogenic differentiation of 3T3-L1 preadipocytes<sup>15,16</sup>. miR-155, miR-221 and miR-222, have also been reported to be the negative regulators of the adipogenic programming of human bone-marrow-derived stromal cells. By contrast, ectopic expression of miR-637, miR-204 and miR-211 induced osteogenesis and at the same time blunted

<sup>1</sup>Collaborative Innovation Center of Tianjin Metabolic Diseases Hospital, Key Laboratory of Hormones and Development (Ministry of Health), Metabolic Diseases Hospital & Institute of Endocrinology, Tianjin Medical University, Tianjin 300070, China. <sup>2</sup>Division of Endocrinology, Tianjin Medical University General Hospital, Tianjin 300052, China. <sup>3</sup>School of Integrative Medicine, Tianjin Traditional Medical University, Tianjin 300193, China. <sup>4</sup>College of Basic Medical Sciences, Tianjin Medical University, Tianjin 300070, China. \*These authors contributed equally to this work. Correspondence and requests for materials should be addressed to B.W. (email: blwang@tmu.edu.cn)

adipogenesis, thus may play a key role in balancing the commitment potential of MSCs. While miR-637 directly targeted osteogenic transcription factor Osterix<sup>17</sup>, miR-204 and its homolog miR-211 functioned via binding the 3'-UTR of another key modulator of osteoblast differentiation, runt-related transcription factor 2 (Runx2)<sup>18</sup>. Our group has recently demonstrated that miR-20a, miR-30e and miR-223 are novel players that contribute to adipogenesis<sup>19–21</sup>.

microRNA-140 (miR-140), generated from the *Mir140* gene, was previously believed to be abundantly and relatively specifically expressed in chondrocytes. The *in vivo* function of miR-140 was demonstrated by Miyaki's group, who created miR-140 knockout and transgenic mice<sup>22</sup>. The miR-140 null mouse had a mild developmental phenotype in the skeleton, potentially via reduced growth plate chondrocyte proliferation, but displayed a premature osteoarthritis phenotype driven at least in part by an increase in expression of *Adamts5*, which was shown to be a direct target of miR-140. Conversely, the transgenic mouse overexpressing miR-140 in cartilage displayed no skeletal phenotype during development but was resistant to antigen-induced arthritis. Recently, miR-140 was identified as a direct downstream component of the BMP4 signaling pathway during the commitment of C3H10T1/2 cells to adipocyte lineage<sup>23</sup>. Overexpression of miR-140 in C3H10T1/2 cells promoted adipocyte differentiation, whereas knockdown of its expression led to impairment of adipogenesis. Further studies suggested that the anti-adipogenic factor osteopetrosis associated transmembrane protein 1 (*Ostm1*) is a bona fide target of miR-140<sup>23</sup>. The authors used a miR-140 precursor expression plasmid that overexpresses both miR-140-5p and miR-140-3p, making it unclear which one was exactly the contributor. At least, one could not exclude the possibility that miR-140-3p might also play a role in adipogenesis since miR-140-3p potentially targets several adipogenic or osteogenic factors like fibroblast growth factor 9 (FGF9), Wnt5 and TGF- $\beta$ 3. Moreover, little is known about the upstream mechanisms that control miR-140-5p expression during adipogenesis. In the present study, we provide novel evidences demonstrating that miR-140-5p is regulated by C/EBP $\alpha$  and is capable of controlling adipogenesis and osteogenesis via direct regulation of transforming growth factor  $\beta$  receptor 1 (Tgfr1).

## Results

**miR-140-5p was upregulated during adipocyte formation.** We previously demonstrated in the microRNA array analysis that the miR-140-5p was increased in primary cultured marrow stromal cells after adipogenic treatment as compared with vehicle treatment<sup>19</sup>. In the current study, we validated the expression profiles of miR-140-5p using qRT-PCR and showed that miR-140-5p was induced by 3-fold 72 h after adipogenic treatment versus vehicle treatment, and reduced by 40% 72 h after osteogenic treatment (Fig. 1a). Moreover, the expression of miR-140-5p was also induced in ST2 cells after adipogenic treatment at all the indicated time points (Fig. 1b). We also checked the level of miR-140-5p expression in ST2 during a full differentiation time course. As illustrated in Fig. 1c, the level of miR-140-5p expression increased dramatically when the cells reached confluence. 1 day after induction, it reached peak and then decreased during terminal adipocyte differentiation. In order to gain insights into the potential biological relevance of miR-140-5p in the regulation of adipose tissue *in vivo*, we examined the expression of miR-140-5p in the genetically obese db/db mice. Compared with the genetically matched lean mice, the expression level of miR-140-5p was increased in both epididymal and inguinal adipose tissue of the db/db mice (Fig. 1d). These results suggested that miR-140-5p might have a regulatory role in adipocyte and/or osteoblast commitment.

**Supplementing miR-140-5p activity in progenitor cells promoted adipocyte differentiation.** The effect of miR-140-5p on the differentiation of stromal ST2 cells was examined. We first examined if miR-140-5p alone could induce differentiation without adipogenic treatment. Supplementing miR-140-5p alone could not promote ST2 cells to differentiate 9 days after transfection (Supplementary Fig. S1a,b). qRT-PCR revealed that it slightly increased the expression of adipogenic factors including PPAR $\gamma$ , adipocyte protein 2 (aP2) and adipisin (Supplementary Fig. S1c).

However, when used in presence of adipogenic agents, miR-140-5p substantially induced adipocyte formation. As shown in Fig. 2, miR-140-5p mimics transfection into ST2 cells led to a significant increase of differentiated adipocyte numbers (52% increase in oil-red O staining compared to control transfection) (Fig. 2a,b). Accordingly, the mRNA levels of adipogenic transcription factors and marker genes, including PPAR $\gamma$ , C/EBP $\alpha$ , aP2 and adipisin, were increased by 2.4, 2.1, 3.4 and 1.7-fold vs. negative control, respectively, 48 h after adipogenic treatment (Fig. 2c). Consistently, the protein levels of PPAR $\gamma$ , C/EBP $\alpha$  and aP2 were increased in ST2 cells 72 h after transfection with miR-140-5p mimics as compared to control mimics transfection (Fig. 2d).

We further demonstrated that miR-140-5p mimics also significantly enhanced adipogenic differentiation from preadipocyte 3T3-L1 cells (75% increase in oil-red O staining compared to control transfection) (Fig. 2e,f). In 3T3-L1 cells, the mRNA levels of PPAR $\gamma$ , C/EBP $\alpha$ , aP2 and adipisin were increased by 1.6, 2.2, 3.8 and 3.2-fold following miR-140-5p transfection as compared to negative control transfection, respectively, 48 h after adipogenic treatment (Fig. 2g). Moreover, miR-140-5p mimics also induced the protein levels of PPAR $\gamma$ , C/EBP $\alpha$  and aP2 72 h after adipogenic treatment as compared to negative control transfection (Fig. 2h).

**Inhibition of endogenous miR-140a-5p reduced adipocyte differentiation.** Transfection of miR-140-5p inhibitor substantially blocked the differentiation of ST2 cells into adipocytes in presence of adipogenic treatment. Oil-red O quantification revealed a 35% decrease after miR-140-5p inhibitor transfection compared to control transfection (Fig. 3a,b). Consistently, the expression levels of the adipogenic factors were all downregulated by the miR-140-5p inhibitor compared to control transfection. Briefly, miR-140-5p inhibitor reduced the mRNA levels of PPAR $\gamma$ , C/EBP $\alpha$ , aP2 and adipisin by 65%, 78%, 51% and 39%, respectively, 48 h after adipogenic treatment (Fig. 3c). The protein levels of PPAR $\gamma$ , c/EBP $\alpha$  and aP2 were substantially decreased in cells transfected with miR-140-5p inhibitor 72 h after adipogenic treatment (Fig. 3d).

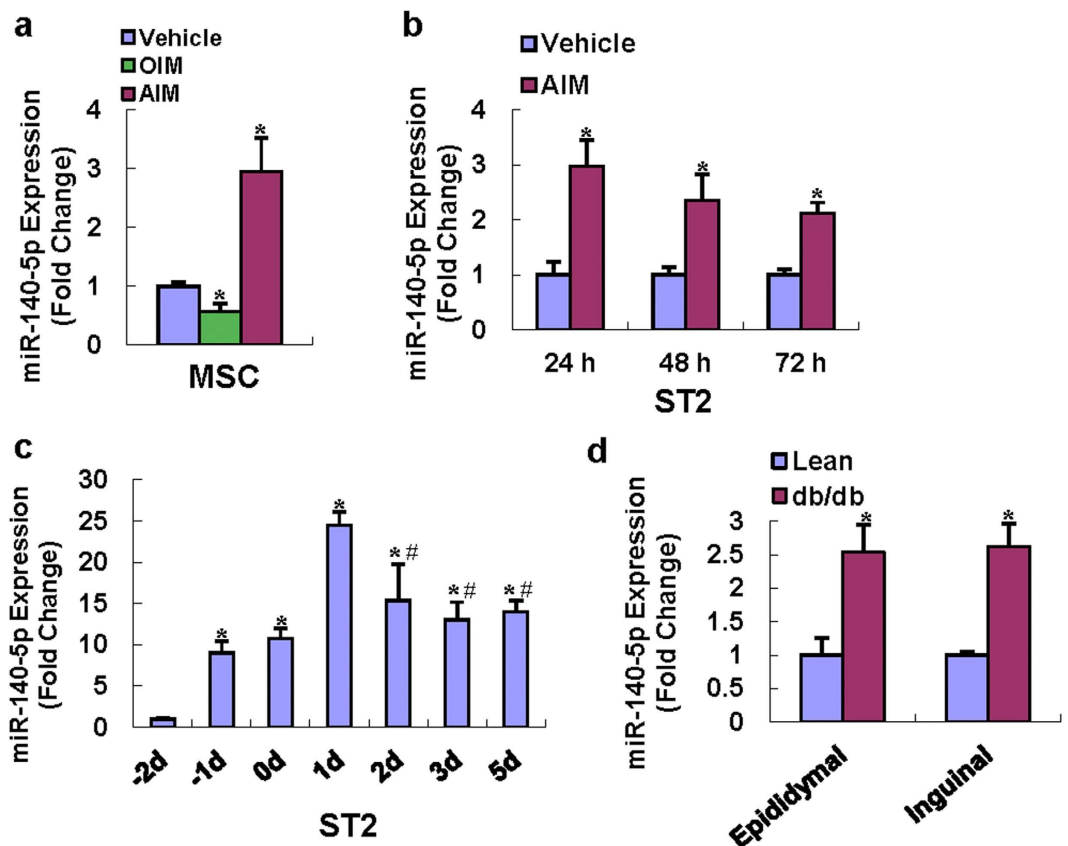


**Figure 1. miR-140-5p was induced during adipocyte formation and reduced during osteoblast differentiation.** qRT-PCR showed that adipogenic treatment (AIM) of primary marrow stromal cells for 72 h induced miR-140-5p, while osteogenic treatment (OIM) reduced miR-140-5p level (a). miR-140-5p was also induced in ST2 24–72 h after treatment with AIM (b). The level of miR-140-5p expression was also checked during a full differentiation time course (c). miR-140-5p expression was analyzed by qRT-PCR in db/db obese mice vs. genetically matched lean mice ( $n = 3$  in each group) (d). Values represent the mean  $\pm$  SD of three experiments. a, b: \*Significant vs. vehicle treatment,  $p < 0.05$ . c: \*Significant vs.  $-2d$ , #Significant vs.  $1d$ ,  $p < 0.05$ . d: \*Significant vs. lean mice,  $p < 0.05$ .

Furthermore, miR-140-5p inhibitor also blocked adipocyte formation from 3T3-L1 cells as compared to control transfection (Fig. 3e,f). Consistently, miR-140-5p inhibitor transfection significantly reduced the mRNA levels of adipogenic factors 48 h after adipogenic treatment, and decreased the protein levels of the adipogenic factors 72 h after adipogenic treatment in 3T3-L1 cells (Fig. 3g,h).

**Inhibition of endogenous miR-140a-5p promoted osteoblast differentiation.** To investigate if miR-140-5p plays a role in regulating osteoblast differentiation, we altered the level of miR-140-5p in stromal ST2 by transfecting the miR-140-5p inhibitor into the cells. Compared to the controls, miR-140-5p inhibitor enhanced alkaline phosphatase (ALP) staining 14 days after osteogenic treatment (Fig. 4a), suggesting the inhibitory role of miR-140-5p in osteoblast differentiation. Consistently, miR-140-5p knockdown significantly promoted the mRNA levels of Runx2, Alp, osteopontin and collagen type I (Col1a1) at day 14 (Fig. 4b).

**Tgfr1 was a direct target of miR-140-5p.** It is well known that miRNAs function through blocking the translation of their target mRNAs. Several regulators of adipocyte and osteoblast differentiation including wntless-type MMTV integration site family member 11 (Wnt11), Tgfr1 and Ostm1 were predicted to be the potential targets of miR-140-5p by using online programs. The reporter constructs of their 3'-UTRs were made and their potential pairings with miR-140-5p are shown in Fig. 5a. There are two potential targeting sites on 3'-UTR of Ostm1, with one conserved among mammals (position 596–603) and the other one not (position 1674–1680) (Fig. 5b). Luciferase assay showed that miR-140-5p mimics significantly reduced the luciferase activity of Wnt11 3'-UTR reporter (Fig. 5c) and Tgfr1 3'-UTR reporter (Fig. 5d) in AD-293 cells compared to negative control. Liu *et al.* demonstrated that the site 1674–1680 of Ostm1 3'-UTR was the direct targeting site of miR-140, but they did not examine the site 596–603<sup>23</sup>. In our study, miR-140-5p mimics also decreased the luciferase activity of the Ostm1 3'-UTR construct with site 1674–1680 but not the construct with 596–603 (Fig. 5e), indicating that the conserved site is a pseudotarget.

These results suggested that Tgfr1 is the direct target of miR-140-5p. Furthermore, supplementing miR-140-5p activity in ST2 cells using the synthetic mimics reduced the level of TGFBR1 protein (Fig. 5f). In contrast,

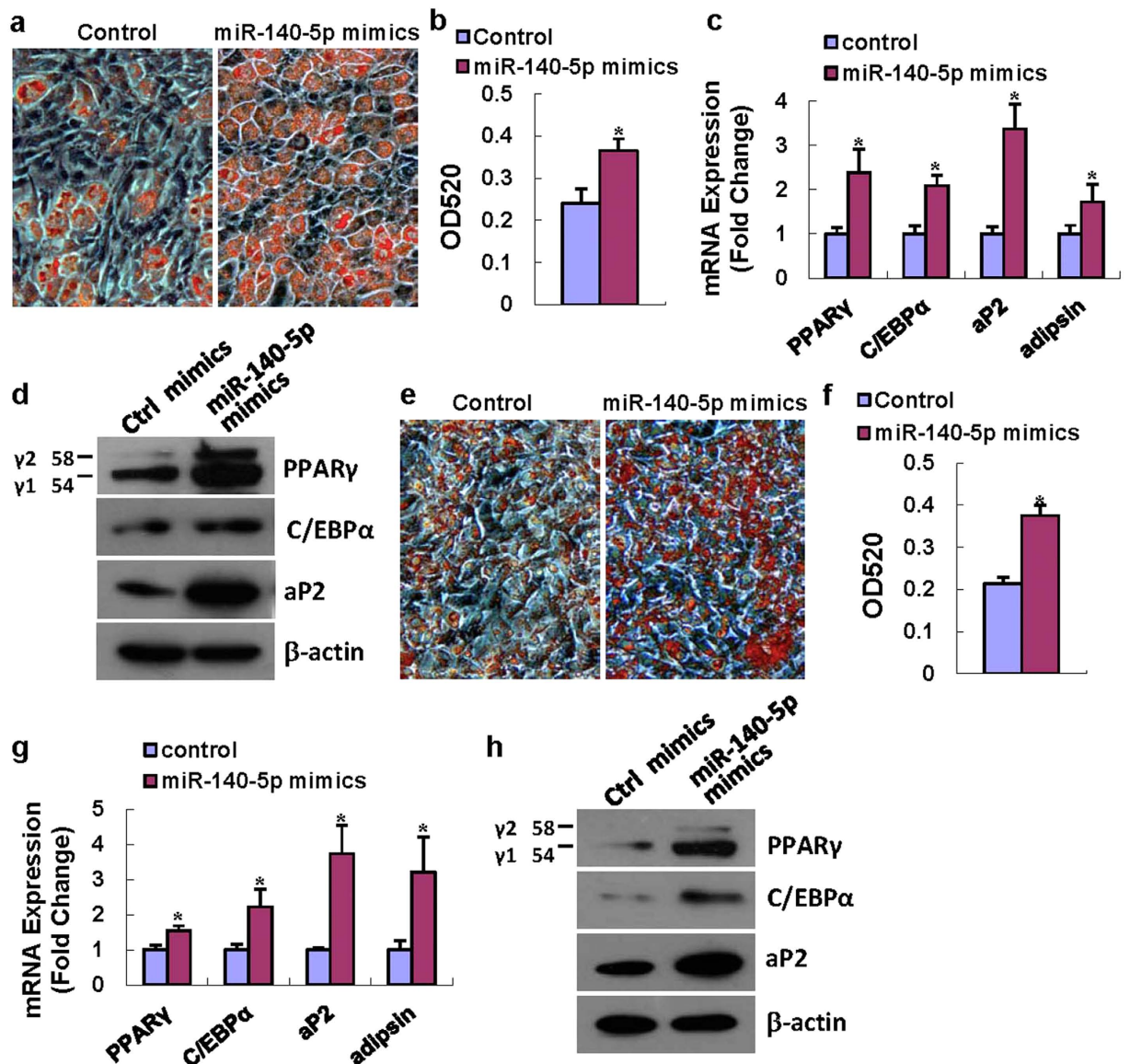


**Figure 2. Supplementing miR-140-5p activity promoted adipocyte differentiation.** miR-140-5p mimics transfection induced adipocyte formation from ST2 in the presence of AIM. Oil-Red O extracted with isopropanol was measured at OD520 (a,b). The mRNA levels of PPAR $\gamma$ , C/EBP $\alpha$ , aP2 and adipsin (c) and protein levels of PPAR $\gamma$ , C/EBP $\alpha$  and aP2 (d) were induced after transfection of miR-140-5p mimics. miR-140-5p mimics also induced adipocyte formation from 3T3-L1 cells (e-h). Values represent the mean  $\pm$  SD of three experiments. \*Significant vs. negative control transfection,  $p < 0.05$ .

suppression of endogenous miR-140-5p using the synthetic inhibitor resulted in an increase of TGFBR1 protein level as compared to control transfection (Fig. 5g).

**Perturbation of Tgfr1 altered adipocyte differentiation.** It is well known that TGF- $\beta$  signaling inhibits adipogenesis *in vitro* and *in vivo*<sup>24</sup>. However, it is unclear whether TGFBR1 directly regulates adipocyte formation from mesenchymal cells. We examined the expression pattern of Tgfr1 during adipocyte formation from ST2 cells. As shown in Fig. 6a, tgfbr1 expression decreased 1 day after adipogenic induction and then increased from day 2 until day 5 when its level restored to normal. We then carried out Tgfr1 gain-of-function and loss-of-function studies. The transfection of the Tgfr1 expression plasmid in ST2 increased Tgfr1 mRNA by 7-fold compared to empty vector transfection (Fig. 6b). In the presence of adipogenic medium, Tgfr1 overexpression significantly inhibited adipocyte formation from ST2 cells (Fig. 6c,d). Consistently, the mRNA levels of PPAR $\gamma$ , C/EBP $\alpha$ , aP2 and adipsin were all decreased upon Tgfr1 overexpression as compared to control transfection (Fig. 6e). The protein levels of PPAR $\gamma$ , C/EBP $\alpha$  and aP2 were also downregulated after Tgfr1 overexpression (Fig. 6f). By contrast, the transfection of the two independent siRNAs targeting different regions of Tgfr1 efficiently downregulated the endogenous mRNA level of Tgfr1, suggesting they work well in the stromal cells (Fig. 6g). Furthermore, in the presence of adipogenic medium, the knockdown of the Tgfr1 level by the two siRNAs dramatically enhanced

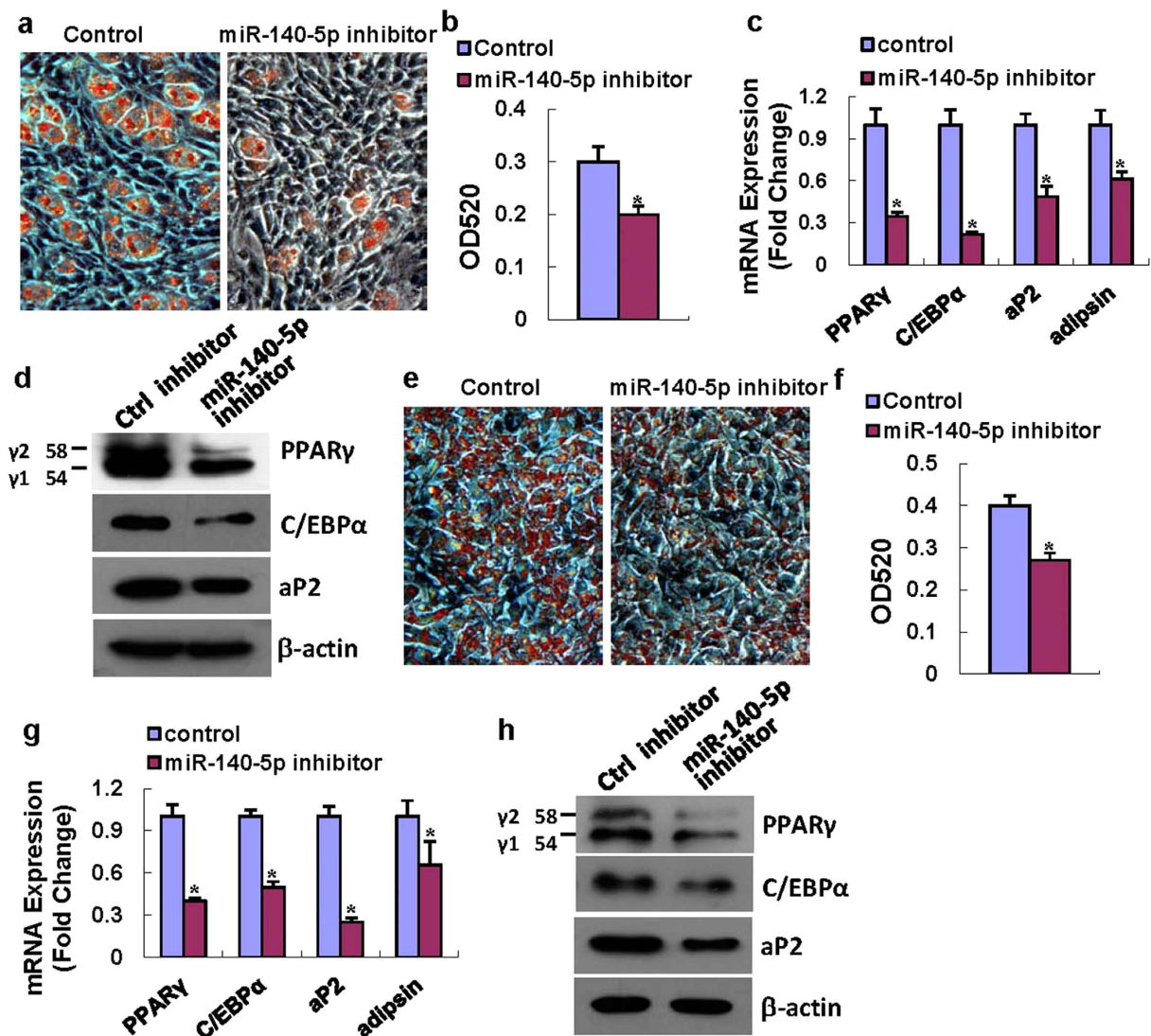


**Figure 3. Inactivation of miR-140-5p reduced adipocyte differentiation.** miR-140-5p inhibitor transfection blocked the adipocyte formation (a,b). Transfection of miR-140-5p inhibitor decreased the mRNA expression levels of PPAR $\gamma$ , C/EBP $\alpha$ , aP2 and adiponectin at 48 h (c), and reduced protein levels of PPAR $\gamma$ , C/EBP $\alpha$  and aP2 at 72 h after adipogenic treatment (d). miR-140-5p inhibitor also inhibited adipocyte formation from 3T3-L1 cells (e-h). Values represent the mean  $\pm$  SD of three experiments. \*Significant vs. negative control transfection,  $p < 0.05$ .

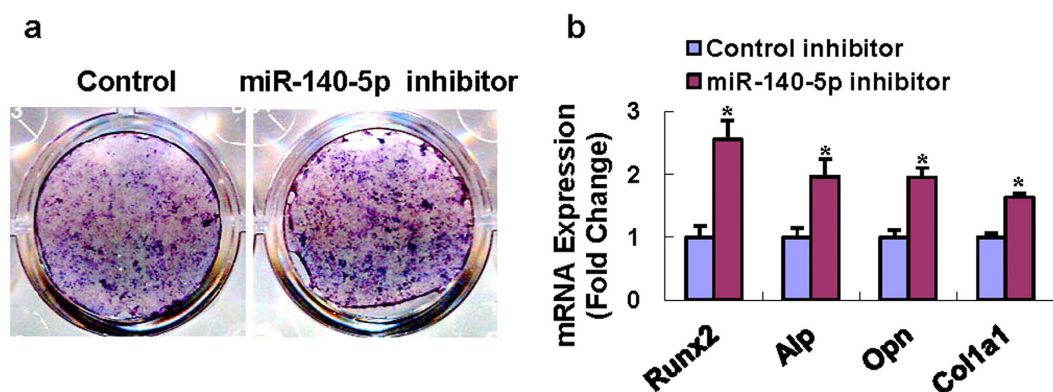


**Figure 4. Inhibition of miR-140-5p in ST2 enhanced osteoblast differentiation.** miR-140-5p inhibitor transfection enhanced ALP staining (a), increased mRNA levels of Runx2, Alp, osteopontin (Opn) and Col1a1 (b) in ST2 cells after osteogenic treatment. \*Significant vs. negative control,  $p < 0.05$ .

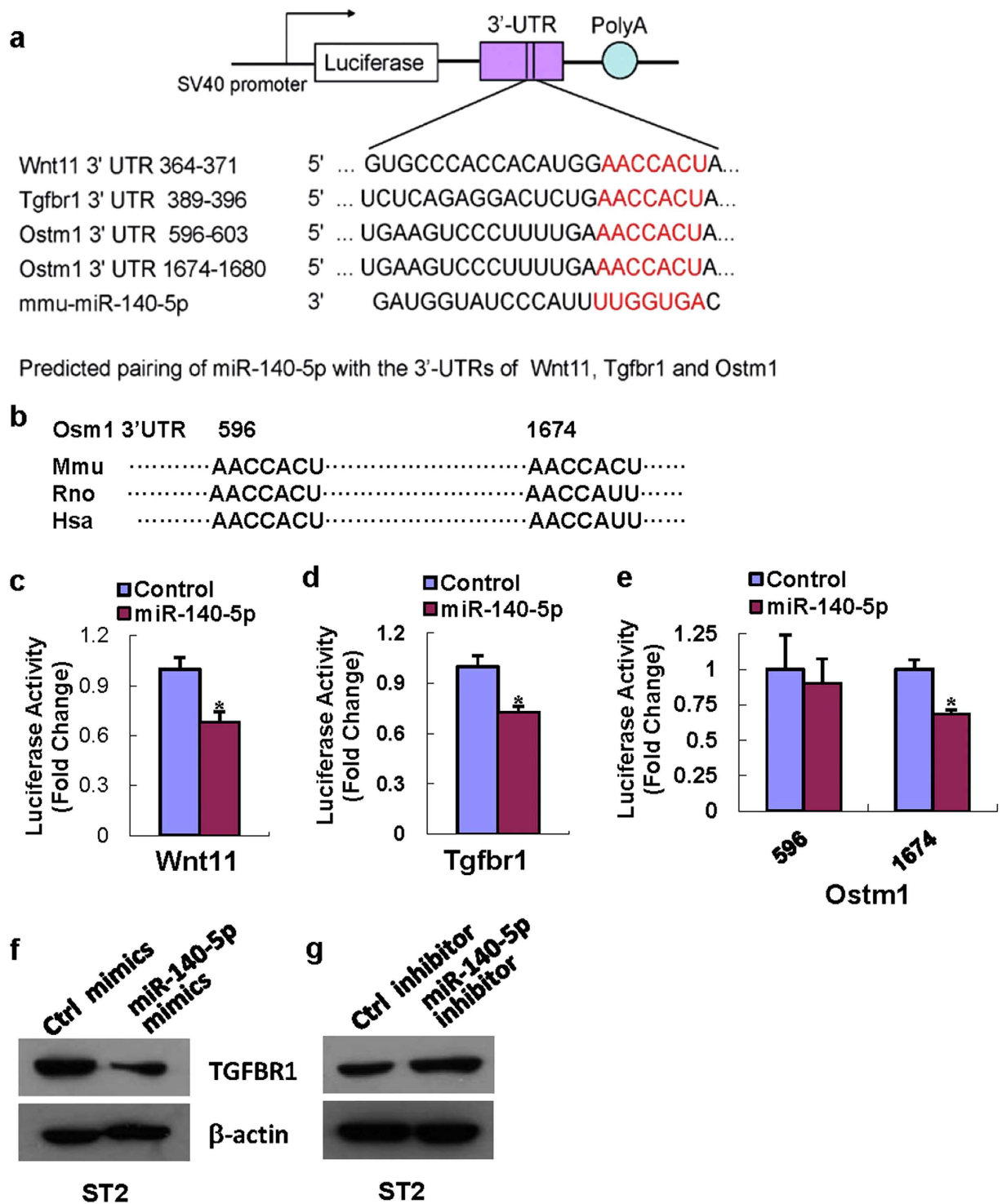


**Figure 5. miR-140-5p directly targeted Tgfr1.** The 3'-UTR fragments of Wnt11, Tgfr1 and Ostm1 were PCR-amplified and cloned (a), and the conservation of the two potential targeting sites on Ostm1 are shown (b). The increase of miR-140-5p in AD-293 decreased the luciferase activity of Wnt11 and Tgfr1 3'-UTR constructs (c,d). It also decreased the luciferase activity of Ostm1 3'-UTR construct with site 1674–1680 but not that with 596–603 (e). miR-140-5p mimics transfection reduced, and miR-140-5p inhibitor transfection induced TGFBR1 protein level in ST2 cells (f,g). Values represent the mean  $\pm$  SD of three experiments. \*Significant vs. control transfection,  $p < 0.05$ .

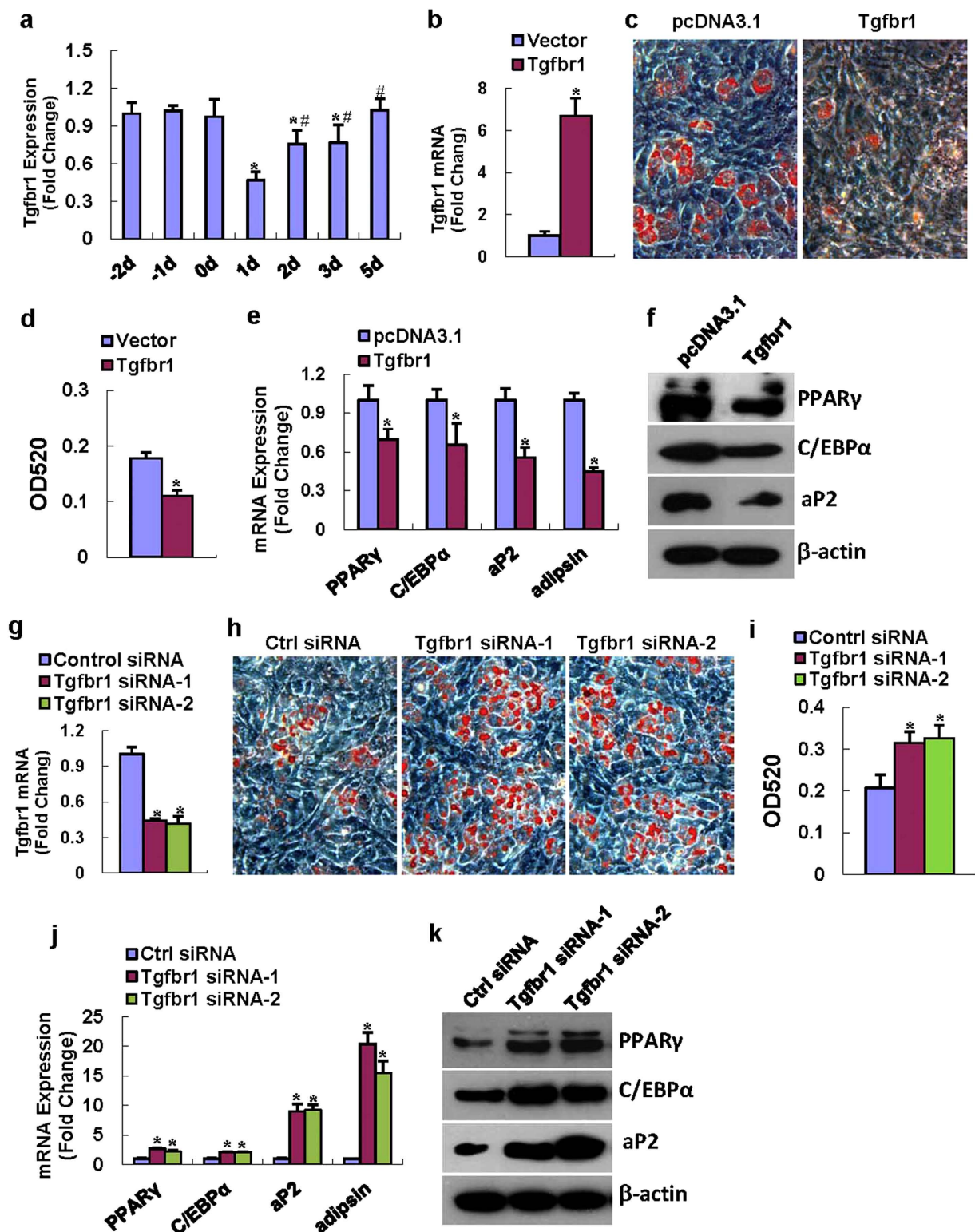


**Figure 6. TGFBR1 negatively regulated adipogenesis.** The mRNA expression pattern of Tgfb1 was examined in ST2 during differentiation (a). The Tgfb1 expression plasmid overexpresses Tgfb1 mRNA in ST2 cells (b). Overexpression of Tgfb1 in ST2 decreased adipocyte formation (c,d). The mRNA and protein levels of PPAR $\gamma$ , C/EBP $\alpha$ , aP2 and adipisin were inhibited (e,h). In contrast, transfection of the two Tgfb1 siRNAs both efficiently knockdown mRNA level of Tgfb1 (g), promoted adipocyte differentiation (h,i), and induced the mRNA and protein levels of PPAR $\gamma$ , C/EBP $\alpha$ , aP2 and adipisin in ST2 cells (j,k). Values represent the mean  $\pm$  SD of three experiments. (a) \*Significant vs. -2 day,  $p < 0.05$ , #Significant vs. 1 day,  $p < 0.05$ ; (b-j) \*Significant vs. control transfection,  $p < 0.05$ .

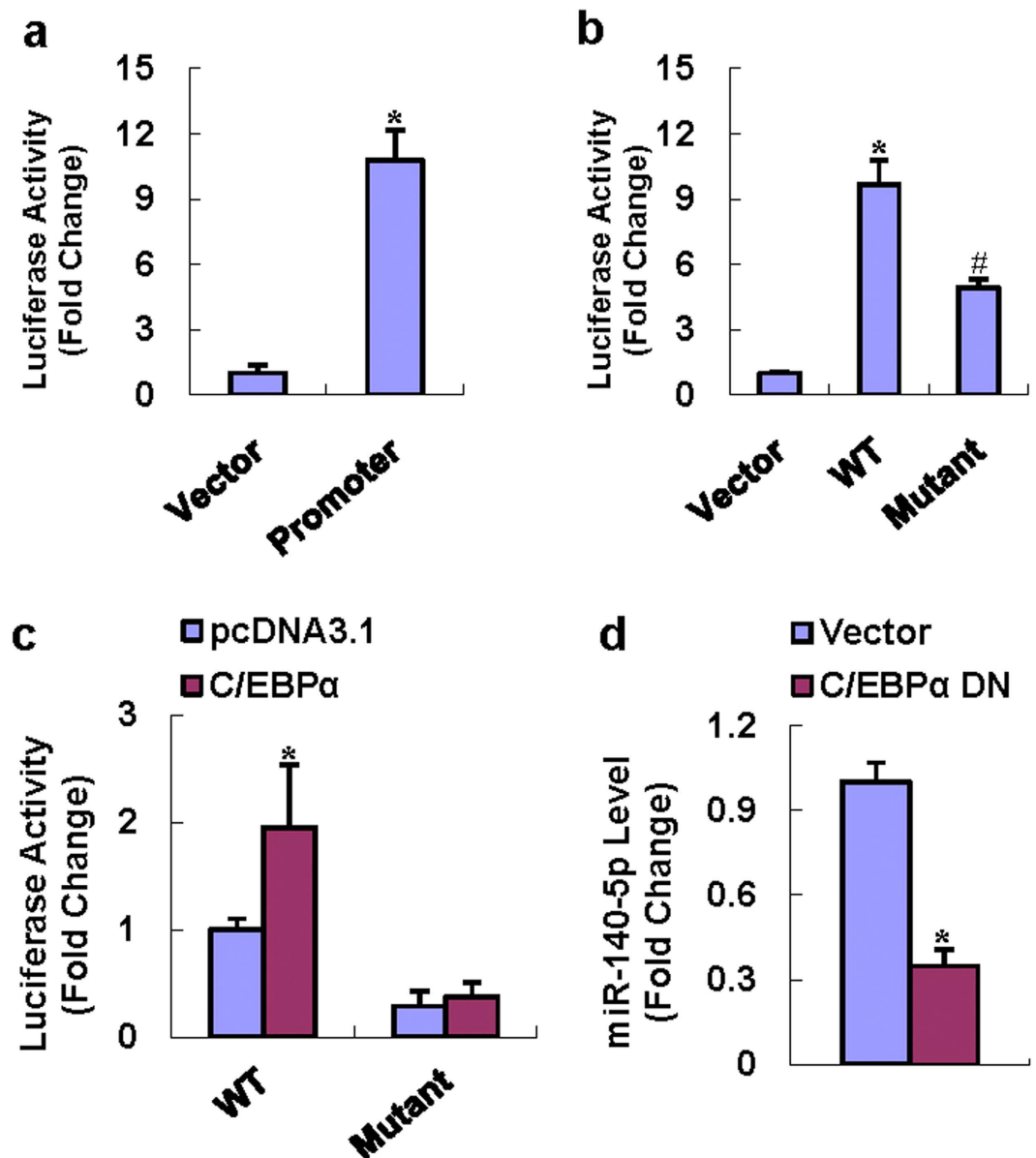


**Figure 7.** C/EBPs transactivated the miR-140-5p promoter. The 1.8-kb promoter fragment of miR-140-5p showed transcriptional activity in 3T3-L1 cells (a). Point mutation of the *miR140/Luc* construct at -281 nt decreased the promoter activity (b). Transfection of C/EBP $\alpha$  enhanced luciferase activity of the WT miR-140-5p promoter construct, but did not affect the mutant construct (c). The transfection of dominant-negative form of C/EBP $\alpha$  decreased the level of miR-140-5p (d). \*Significant vs. empty vector,  $p < 0.05$ ; #Significant vs. WT promoter,  $p < 0.05$ .

formation of oil-red O positive adipocytes as compared to control siRNA transfection (Fig. 6h,i). The mRNA and protein levels of the adipogenic factors were substantially enhanced following Tgfb $\beta$ 1 knockdown by the two siRNAs (Fig. 6j,k).

**C/EBPs regulated miR-140-5p expression in mesenchymal progenitor cell.** To clarify the mechanisms that might regulate miR-140-5p expression, the promoter construct of miR-140-5p was made as described by Yang<sup>25</sup>. As shown in Fig. 7a, the promoter construct *miR140/Luc* had transcriptional activity in 3T3-L1 cells, showing 11-fold increase vs. the promoterless pGL3-basic. The prediction of transcription factor binding sites was performed with TFSEARCH (<http://www.cbrc.jp/research/db/TFSEARCH.html>) and TFBIND (<http://tfbind.hgc.jp/>), which revealed a putative C/EBP binding motif within the proximal promoter at -281 nt (CCCTTTCACCAGCC) (Fig. 7B), indicating that miR-140-5p might be regulated by C/EBPs. To assess the importance of the putative C/EBP binding site we made the point mutation within the *miR140/Luc* promoter reporter construct. The removal of the C/EBP binding site significantly reduced the transcriptional activity of the promoter (Fig. 7b). We further

investigated whether C/EBPs activate the miR-140-5p promoter at the putative site. C/EBP $\alpha$  significantly induced the transcriptional activity of the WT promoter construct, while had no effect on the mutant promoter construct (Fig. 7c). Consistent to this, transfection of the dominant-negative construct of C/EBP $\alpha$  significantly decreased the expression level of miR-140-5p in 3T3-L1 cells 72 h after transfection (Fig. 7d).

## Discussion

In the present study, we found that the expression of miR-140-5p was increased either *in vitro* in stromal cells during adipogenesis, or *in vivo* in adipose tissue of db/db obese mice. Moreover, it was decreased in primary stromal cells during osteogenesis, suggesting that miR-140-5p might play a role in adipogenesis and/or osteogenesis.

To delineate the precise role of miR-140-5p in cell fate decision, we tested the effects of miR-140-5p on adipocyte differentiation. Our data showed that supplementing miR-140-5p in undifferentiated adipogenic progenitors using synthetic miR-140-5p mimics potentiated the formation of adipocytes in presence of adipogenic treatment. Conversely, inactivating miR-140-5p in adipogenic progenitors using miR-140-5p inhibitor blocked differentiation of adipocytes. Concomitantly, knockdown of miR-140-5p using the inhibitor in stromal ST2 potentiated osteoblast differentiation. These findings provided evidences that miR-140-5p reciprocally regulates adipocyte and osteoblast differentiation from progenitor cells.

miRNAs finely modulate osteoblast/adipocyte differentiation through their direct targeting of diverse signaling molecules and pathways that include bone morphogenetic protein 2 (BMP2)/Smad, Wnt/ $\beta$ -catenin and Runx2 signaling pathways<sup>26–29</sup>. In an attempt to gain more insights into the regulatory mechanisms that control adipocyte differentiation by miR-140-5p, we analysed the potential targets using Targetscan, PicTar, and miRDB. Several important factors that might have contributions to the differentiation of osteoblast and/or adipocyte, i.e., Wnt11, Tgfr1 and Ostm1, were predicted as the potential targets. Liu *et al.* demonstrated that the poorly conserved site 1674–1680 of Ostm1 3' UTR was the direct targeting site of miR-140<sup>23</sup>. In our study, we also demonstrated miR-140-5p targeted this site but not the conserved site 596–603, indicating that the conserved site is a pseudotarget. The luciferase assay in our study also showed that miR-140-5p altered the luciferase activity of the 3' UTR reporters of Wnt11 and Tgfr1, suggesting they are the direct targets.

Wnt11 signals through both canonical and noncanonical pathways<sup>30</sup> and is up-regulated during osteoblast differentiation and fracture healing<sup>31</sup>. Friedman *et al.* demonstrated that Wnt11 overexpression in preosteoblast increases  $\beta$ -catenin accumulation and promotes bone morphogenetic protein (BMP)-induced expression of alkaline phosphatase and mineralization<sup>32</sup>. Moreover, Wnt11 increases expression of R-spondin 2 (Rspo2), a secreted factor known to enhance Wnt signaling. The study concluded that Wnt11 signals to activate osteoblast differentiation through  $\beta$ -catenin, and Rspo2 expression<sup>32</sup>.

Of note, Wnt11 mRNA remains at a quite low expression level in the adipogenic cell lines we used before and after adipogenic treatment (data not shown). Thus it might not be critical during adipogenesis. By contrast, Tgfr1 has much higher expression level in the adipogenic cell lines (data not shown). Furthermore, supplementing miR-142-5p in ST2 cells reduced, while silencing miR-142-5p induced the protein levels of TGFBR1. These data identified Tgfr1 as a direct target of miR-140-5p.

TGF- $\beta$  can provide competence for early stages of chondroblastic and osteoblastic differentiation, but it inhibits adipogenesis and late-stage osteogenesis<sup>24,33</sup>. TGF- $\beta$  signaling begins with binding of TGF- $\beta$  ligands to type II serine/threonine kinase receptor termed TGFBR2, which then phosphorylates and activates type I serine/threonine kinase receptor. The activated type I receptor activates Smad proteins that regulate transcription. Up to now, it is unclear whether TGFBR1 directly regulates adipocyte formation from mesenchymal cells. In the present study, we demonstrated TGFBR1 acts as a player in adipogenesis in murine progenitor cells. The knockdown of Tgfr1 in the stromal ST2 cells enhanced the differentiation into mature adipocytes. By contrast, enforced expression of Tgfr1 in ST2 blocked adipocyte differentiation. These data provide evidences that the cell fate decision of miR-140-5p may depend upon its inhibitory effect on TGF- $\beta$  signaling, hence driving the progenitor cells to differentiate into adipocytes.

To gain further insight into the control of miR-140-5p expression and function, we cloned the promoter of miR-140-5p and examined cis-acting elements within the proximal promoter using TFSEARCH and TFBIND programs and found a potential binding site for C/EBPs within the proximal promoter. In our study, the WT promoter construct that harbored the C/EBP binding sequence showed transcriptional activity in 3T3-L1 cells, which was further stimulated following C/EBP $\alpha$  overexpression. Consistently, dominant negative form of C/EBP $\alpha$  downregulated the expression level of miR-140-5p. Moreover, point mutation of the C/EBP binding sequence at –281 nt was made and the mutant construct showed less transcriptional activity. Of more interest, the mutant failed to respond to C/EBP $\alpha$  transcription factor. We thus draw the conclusion that C/EBPs bind to the proximal promoter of miR-140-5p to positively regulate the expression of miR-140-5p.

The data we have shown in this paper tends to develop a model for miR-140-5p expression and function. Adipogenic signals lead to the activation of C/EBPs transcription factors in progenitor cells. In addition to working together with PPAR $\gamma$  to induce the coding genes essential for adipocyte differentiation, C/EBPs may also transactivate miR-140-5p promoter to increase the miR-140-5p level. In turn, miR-140-5p may further promote adipocyte differentiation and maintain the levels of C/EBPs mRNA and protein levels via repressing TGFBR1. Thus, we propose that a unique autoregulatory feedback loop exists among C/EBPs, miR-140-5p and TGFBR1. The current study also suggests that miR-140-5p is an attractive potential target for new therapies aimed at controlling metabolic disorders like osteoporosis and obesity.

## Methods

**Mice.** 10-week-old db/db mice and their genetically matched lean littermates were purchased from Model Animal Research Center of Nanjing University (Nanjing, China). RNA was extracted from epididymal and inguinal adipose tissue. qRT-PCR was done to examine the expression level of miR-140-5p. All the experiments involving

animals were carried out in accordance with the Chinese guidelines for animal welfare and experimental protocol, and were approved by the Animal Care and Use Committee of the Metabolic Diseases Hospital, Tianjin Medical University.

**Cells.** Bone marrow stromal cells were isolated from femurs and tibiae of 4-week-old C57 mice and cultured in  $\alpha$ -MEM containing 10% FBS in 25 cm<sup>2</sup> flasks as previously described<sup>19,34</sup>. For osteogenic differentiation, 80% confluent cells were treated with osteogenic medium (OIM,  $\alpha$ -MEM containing 10% FBS, 50  $\mu$ g/mL ascorbic acid and 5 mmol/L  $\beta$ -glycerophosphate) for 3 days followed by miRNA isolation. For adipogenic differentiation, confluent cells were cultured in adipogenic medium (AIM,  $\alpha$ -MEM containing 10% FBS, 0.5  $\mu$ M dexamethasone, 0.25 mM methylisobutylxanthine, 5  $\mu$ g/ml insulin, and 50  $\mu$ M indomethacin) for 3 days followed by miRNA isolation.

3T3-L1 and ST2 cells were maintained in DMEM supplemented with 10% FBS. When the cells reached 100% confluence, AIM was added to induce adipocyte formation. When ST2 cells reached 80% confluence, OIM was added to induce osteoblast differentiation.

**Quantitative RT-PCR.** We previously examined the miRNA expression profiles in primary cultured marrow stromal cells after adipogenic and osteogenic treatment<sup>19</sup>. In this study, we validated the expression levels of miR-140-5p by using a qRT-PCR system (Genecopoeia, Germantown, MD)<sup>35</sup>. Briefly, RNA was extracted using a miRNA isolation kit (Omega Bio-Tek, Norcross, GA, USA). 1  $\mu$ g RNA was reverse-transcribed into cDNA using the RT primer. Subsequently, miRNAs were PCR-amplified on a real time fluorescent PCR cycler using specific forward primers and a universal reverse primer. The qRT-PCR consisted of 40 cycles (95 °C for 10 s, 60 °C for 10 s, and 72 °C for 10 s) after an initial denaturing step (95 °C for 2 min). The expression levels were normalized against U6, and measured by the comparative Ct ( $\Delta\Delta$ Ct) method<sup>36</sup>.

For mRNA expression analysis, total cellular RNA was isolated and reverse transcribed to cDNA. Real-time PCR amplifications were performed using SYBR green real-time PCR kit (Shenggong Biotech Company, Shanghai, China). The primers are listed in Supplementary Table 1. The expression levels of the target genes were normalized to that of  $\beta$ -actin.

**Transfections.** 50 nM mimics or 75 nM inhibitor of miR-140-5p (Genepharma, Shanghai, China) was transfected into cell cultures using lipofectamine RNAi-max (Invitrogen, Carlsbad, CA, USA) to activate or inactivate miR-140-5p activity, respectively. Negative controls (Scramble) were used for both reactions. 12 h following transfection, the transfection medium was replaced with complete medium and was then replaced with AIM when the cells reached 100% confluence to induce adipocyte differentiation. 48 h following adipogenic treatment, the cells were subjected to RNA extraction and qRT-PCR analysis. 72 h following adipogenic treatment, the cells were subjected to protein isolation and Western blotting analysis. For oil-red O staining, the cells were treated with AIM for 72 h, then with insulin alone for additional 48 h.

For the Tgfr1 loss of function study, we transfected ST2 cells for 12 h with either 30 nmol/L Tgfr1 siRNAs or negative control siRNA (Genepharma, Shanghai, China) using lipofectamine RNAi-max. For the Tgfr1 gain of function studies, the ST2 cells were transfected with Tgfr1 expression plasmid or the empty vector for 12 h using lipofectamine 3000 (Invitrogen, Carlsbad, CA, USA). AIM was added to the cultures to allow the cells to differentiate when reaching 100% confluence.

**Constructs and luciferase reporter assay.** The online programs TargetScan (<http://www.targetscan.org/>), PicTar (<http://pictar.mdc-berlin.de/>) and miRDB ([mirdb.org/miRDB](http://mirdb.org/miRDB)) were used to predict the potential target genes of miR-140-5p. We PCR-amplified the 3'-UTR sequences of the potential target genes carrying the putative miR-140-5p binding sites using mouse DNA as a template. The primers are listed in Supplementary Table 2. The PCR products were subcloned into a modified pGL3-control vector<sup>19</sup> at EcoRI/EcoRV sites. 293-AD cells were cotransfected with miR-140-5p mimics or its negative control along with the 3'-UTR construct in 24-well plates. The Renilla luciferase reporter plasmid pRL-SV40 (10 ng) was also included in the cotransfection mixture. The cells were harvested, lysed and subjected to luciferase assay 36 h after transfection using a dual-luciferase reporter assay kit (Promega, San Luis Obispo, CA, USA). The relative luciferase activity was calculated by normalizing the Firefly luciferase activity to the Renilla luciferase activity.

For the miR-140-5p promoter study, the wild-type mouse miR-140-5p promoter construct (*miR140/Luc*) was made as described by Yang<sup>25</sup>. The primers are listed in Supplementary Table 2. The DNA fragment obtained by PCR was inserted into pGL3-basic at *KpnI* and *HindIII* sites, respectively. Point mutation to the C/EBP binding sequence (−281nt, CCCTTTCACCAGCC) was made. To study the involvement of C/EBPs in the regulation, the wild-type or mutant miR-140-5p promoter construct was co-transfected with C/EBP $\alpha$  expression plasmid (addgene, Cambridge, MA), or the empty vector into 3T3-L1 cells using lipofectamine 3000 reagent. pRL-SV40 was also included in the co-transfection mixture. 36 h after transfection, the cell extracts were harvested and the luciferase activity was measured.

**Oil-red O staining.** Fully differentiated adipocytes were gently washed twice with phosphate-buffered saline (PBS), and then fixed in 4% paraformaldehyde for 10 min. The samples were then washed twice with deionized water, and staining was carried out in 60% saturated oil-red O solution for 5 min. For oil-red O quantification, isopropanol was added to each well. Light absorbance was measured at 520 nm.

**ALP Staining.** The ST2 cells were cultured for 14 days followed by alkaline phosphatase (ALP) staining as described in previous studies<sup>37</sup>. In brief, cells were fixed in 10% formalin for 10 min and stained using 1-Step™ NBT/BCIP staining kit (Pierce, Thermo Scientific, Rockford, IL, USA) for 15 min.

**Western blot analysis.** Cells were lysed and proteins were separated by SDS-PAGE and transferred onto nitrocellulose membrane. The membranes were incubated overnight with rabbit monoclonal anti-C/EBP $\alpha$ , (Abcam, Cambridge, MA), rabbit polyclonal anti-TGFBR1 (Abgent, San Diego, CA), rabbit polyclonal anti-PPAR $\gamma$ , anti-aP2, or anti- $\beta$ -actin antibodies (Proteintech, Wuhan, China). This was then followed by incubation with the corresponding horseradish peroxidase-labeled IgG (1:3000) for 1 h. Finally, chemiluminescence reagent (Advanta, Menlo Park, California) was used to visualize the results.

**Statistical analysis.** Data are expressed as mean  $\pm$  SD. For the relative mRNA and luciferase activity quantification, the means of the control groups are set to 1. Statistical analysis was performed using the independent t test. A p value of  $< 0.05$  was considered to be statistically significant.

## References

- Abdallah, B. M., Jafari, A., Zaher, W., Qiu, W. & Kassem, M. Skeletal (stromal) stem cells: an update on intracellular signaling pathways controlling osteoblast differentiation. *Bone* **70**, 28–36, doi: 10.1016/j.bone.2014.07.028 (2015).
- Tontonoz, P., Hu, E. & Spiegelman, B. M. Stimulation of adipogenesis in fibroblasts by PPAR gamma 2, a lipid-activated transcription factor. *Cell* **79**, 1147–1156, doi: 0092-8674(94)90006-X (1994).
- Siersbaek, R., Nielsen, R. & Mandrup, S. Transcriptional networks and chromatin remodeling controlling adipogenesis. *Trends Endocrinol Metab* **23**, 56–64, doi: 10.1016/j.tem.2011.10.001 (2012).
- Lin, F. T. & Lane, M. D. CCAAT/enhancer binding protein alpha is sufficient to initiate the 3T3-L1 adipocyte differentiation program. *Proc Natl Acad Sci USA* **91**, 8757–8761 (1994).
- Zanotti, S., Stadmeier, L., Smerdel-Ramoya, A., Durant, D. & Canalis, E. Misexpression of CCAAT/enhancer binding protein beta causes osteopenia. *J Endocrinol* **201**, 263–274, doi: 10.1677/JOE-08-0514 (2009).
- Akune, T. *et al.* PPARgamma insufficiency enhances osteogenesis through osteoblast formation from bone marrow progenitors. *J Clin Invest* **113**, 846–855, doi: 10.1172/JCI19900 (2004).
- Zhang, J. *et al.* Selective disruption of PPARgamma 2 impairs the development of adipose tissue and insulin sensitivity. *Proc Natl Acad Sci USA* **101**, 10703–10708, doi: 10.1073/pnas.0403652101 (2004).
- Smink, J. J. & Leutz, A. Instruction of mesenchymal cell fate by the transcription factor C/EBPbeta. *Gene* **497**, 10–17, doi: 10.1016/j.gene.2012.01.043 (2012).
- Freytag, S. O., Paielli, D. L. & Gilbert, J. D. Ectopic expression of the CCAAT/enhancer-binding protein alpha promotes the adipogenic program in a variety of mouse fibroblastic cells. *Genes Dev* **8**, 1654–1663 (1994).
- Linhardt, H. G. *et al.* C/EBPalpha is required for differentiation of white, but not brown, adipose tissue. *Proc Natl Acad Sci USA* **98**, 12532–12537, doi: 10.1073/pnas.211416898 (2001).
- Wang, N. D. *et al.* Impaired energy homeostasis in C/EBP alpha knockout mice. *Science* **269**, 1108–1112 (1995).
- Tanaka, T., Yoshida, N., Kishimoto, T. & Akira, S. Defective adipocyte differentiation in mice lacking the C/EBPbeta and/or C/EBPdelta gene. *EMBO J* **16**, 7432–7443, doi: 10.1093/emboj/16.24.7432 (1997).
- Ryoo, H. M., Lee, M. H. & Kim, Y. J. Critical molecular switches involved in BMP-2-induced osteogenic differentiation of mesenchymal cells. *Gene* **366**, 51–57, doi: 10.1016/j.gene.2005.10.011 (2006).
- Wang, Y. *et al.* Wnt and the Wnt signaling pathway in bone development and disease. *Front Biosci (Landmark Ed)* **19**, 379–407, doi: 4214 (2014).
- Lin, Q., Gao, Z., Alarcon, R. M., Ye, J. & Yun, Z. A role of miR-27 in the regulation of adipogenesis. *FEBS J* **276**, 2348–2358 (2009).
- Kim, S. Y. *et al.* miR-27a is a negative regulator of adipocyte differentiation via suppressing PPARgamma expression. *Biochem Biophys Res Commun* **392**, 323–328, doi: 10.1016/j.bbrc.2010.01.012 (2010).
- Zhang, J. F. *et al.* MiR-637 maintains the balance between adipocytes and osteoblasts by directly targeting Osterix. *Mol Biol Cell* **22**, 3955–3961, doi: 10.1091/mbc.E11-04-0356 (2011).
- Huang, J., Zhao, L., Xing, L. & Chen, D. MicroRNA-204 regulates Runx2 protein expression and mesenchymal progenitor cell differentiation. *Stem Cells* **28**, 357–364, doi: 10.1002/stem.288 (2010).
- Wang, J. *et al.* miR-30e reciprocally regulates the differentiation of adipocytes and osteoblasts by directly targeting low-density lipoprotein receptor-related protein 6. *Cell Death Dis* **4**, e845, doi: 10.1038/cddis.2013.356 (2013).
- Zhou, J. *et al.* miR-20a regulates adipocyte differentiation by targeting lysine-specific demethylase 6b and transforming growth factor-beta signaling. *Int J Obes (Lond)* **39**, 1282–1291, doi: 10.1038/ijo.2015.43 (2015).
- Guan, X. *et al.* miR-223 Regulates Adipogenic and Osteogenic Differentiation of Mesenchymal Stem Cells Through a C/EBPs/miR-223/FGFR2 Regulatory Feedback Loop. *Stem Cells* **33**, 1589–1600, doi: 10.1002/stem.1947 (2015).
- Miyaki, S. *et al.* MicroRNA-140 plays dual roles in both cartilage development and homeostasis. *Genes Dev* **24**, 1173–1185, doi: 10.1101/gad.1915510 (2010).
- Liu, Y. *et al.* MicroRNA-140 promotes adipocyte lineage commitment of C3H10T1/2 pluripotent stem cells via targeting osteopetrosis-associated transmembrane protein 1. *J Biol Chem* **288**, 8222–8230, doi: 10.1074/jbc.M112.426163 (2013).
- Roelen, B. A. & Dijke, P. Controlling mesenchymal stem cell differentiation by TGFbeta family members. *J Orthop Sci* **8**, 740–748, doi: 10.1007/s00776-003-0702-2 (2003).
- Yang, J. *et al.* MiR-140 is co-expressed with Wwp2-C transcript and activated by Sox9 to target Sp1 in maintaining the chondrocyte proliferation. *FEBS Lett* **585**, 2992–2997, doi: 10.1016/j.febslet.2011.08.013 (2011).
- Hu, R. *et al.* A Runx2/miR-3960/miR-2861 regulatory feedback loop during mouse osteoblast differentiation. *J Biol Chem* **286**, 12328–12339, doi: 10.1074/jbc.M110.176099 (2011).
- Kim, E. J., Kang, I. H., Lee, J. W., Jang, W. G. & Koh, J. T. MiR-433 mediates ERRgamma-suppressed osteoblast differentiation via direct targeting to Runx2 mRNA in C3H10T1/2 cells. *Life Sci* **92**, 562–568, doi: 10.1016/j.lfs.2013.01.015 (2013).
- Hassan, M. Q. *et al.* miR-218 directs a Wnt signaling circuit to promote differentiation of osteoblasts and osteomimicry of metastatic cancer cells. *J Biol Chem* **287**, 42084–42092, doi: 10.1074/jbc.M112.377515 (2012).
- Luzi, E. *et al.* Osteogenic differentiation of human adipose tissue-derived stem cells is modulated by the miR-26a targeting of the SMAD1 transcription factor. *J Bone Miner Res* **23**, 287–295, doi: 10.1359/jbmr.071011 (2008).
- Tao, Q. *et al.* Maternal wnt11 activates the canonical wnt signaling pathway required for axis formation in Xenopus embryos. *Cell* **120**, 857–871, doi: 10.1016/j.cell.2005.01.013 (2005).
- Boland, G. M., Perkins, G., Hall, D. J. & Tuan, R. S. Wnt 3a promotes proliferation and suppresses osteogenic differentiation of adult human mesenchymal stem cells. *J Cell Biochem* **93**, 1210–1230, doi: 10.1002/jcb.20284 (2004).
- Friedman, M. S., Oyserman, S. M. & Hankenson, K. D. Wnt11 promotes osteoblast maturation and mineralization through R-spondin 2. *J Biol Chem* **284**, 14117–14125, doi: 10.1074/jbc.M808337200 (2009).
- Maeda, S., Hayashi, M., Komiya, S., Imamura, T. & Miyazono, K. Endogenous TGF-beta signaling suppresses maturation of osteoblastic mesenchymal cells. *EMBO J* **23**, 552–563, doi: 10.1038/sj.emboj.7600067 (2004).
- Anjos-Afonso, F. & Bonnet, D. Isolation, culture, and differentiation potential of mouse marrow stromal cells. *Curr Protoc Stem Cell Biol* Chapter 2, Unit 2B 3, doi: 10.1002/9780470151808.sc02b03s7 (2008).

35. Chen, C. *et al.* Real-time quantification of microRNAs by stem-loop RT-PCR. *Nucleic Acids Res* **33**, e179, doi: 33/20/e179 (2005).
36. Livak, K. J. & Schmittgen, T. D. Analysis of relative gene expression data using real-time quantitative PCR and the 2<sup>-Delta Delta</sup> C(T) Method. *Methods* **25**, 402–408, doi: 10.1006/meth.2001.1262 (2001).
37. Zhao, M. *et al.* Smurf1 inhibits osteoblast differentiation and bone formation *in vitro* and *in vivo*. *J Biol Chem* **279**, 12854–12859, doi: 10.1074/jbc.M313294200 (2004).

### Acknowledgements

This work was supported by grants No. 81472040 and 81271977 from Natural Science Foundation of China and by grants No. 11JCZDJC16500 from Tianjin Municipal Science and Technology Commission.

### Author Contributions

X.Z., A.C., Y.L., Y.G. and H.W. performed experiments. Z.M., X.L. and B.W. conceived of the study and supervised the work. B.W. analyzed data and drafted the manuscript. All authors approved the final version of the manuscript to be published.

### Additional Information

**Supplementary information** accompanies this paper at <http://www.nature.com/srep>

**Competing financial interests:** The authors declare no competing financial interests.

**How to cite this article:** Zhang, X. *et al.* miR-140-5p regulates adipocyte differentiation by targeting transforming growth factor- $\beta$  signaling. *Sci. Rep.* **5**, 18118; doi: 10.1038/srep18118 (2015).



This work is licensed under a Creative Commons Attribution 4.0 International License. The images or other third party material in this article are included in the article's Creative Commons license, unless indicated otherwise in the credit line; if the material is not included under the Creative Commons license, users will need to obtain permission from the license holder to reproduce the material. To view a copy of this license, visit <http://creativecommons.org/licenses/by/4.0/>